

Molecular Properties of Coordination Compounds of the Croconate Ion with First-Row Divalent Transition Metals: a Quantum Mechanical Study

D. E. C. Ferreira,^a H. F. Dos Santos,^b W. B. De Almeida^a and G. M. A. Junqueira^{*,b,c}

^aDepartamento de Química, Instituto de Ciências Exatas, Universidade Federal de Minas Gerais, 31270-901 Belo Horizonte-MG, Brazil

^bDepartamento de Química, Instituto de Ciências Exatas, Universidade Federal de Juiz de Fora, 36036-900 Juiz de Fora-MG, Brazil

^cDepartamento de Química, Universidade de Coimbra, 3004-535 Coimbra, Portugal

Neste artigo são relatadas geometrias, propriedades magnéticas e espectroscópicas de complexos de croconato $[M(C_5O_5)(H_2O)_4]$ ($M = Mn^{2+}, Fe^{2+}, Co^{2+}, Ni^{2+}, Cu^{2+}$ e Zn^{2+}), calculados com Teoria do Funcional de Densidade. O estado fundamental de todos os complexos obtido foi de alto spin, em acordo com a proposta experimental. As estruturas e frequências vibracionais calculadas também estão em acordo com o experimento, embora as comparações feitas sejam com estruturas do estado sólido. As propriedades ópticas não lineares (ONL) foram calculadas para todos os compostos analisados, usando o método *Time Dependent Hartree-Fock* (TDHF) dentro da abordagem estática, sugerindo que estes complexos de metais de transição possam ser utilizados no desenvolvimento de novos materiais baseados em moléculas.

In this paper we report geometries, magnetic and vibrational spectroscopic properties of croconate complexes $[M(C_5O_5)(H_2O)_4]$ ($M = Mn^{2+}, Fe^{2+}, Co^{2+}, Ni^{2+}, Cu^{2+}$ and Zn^{2+}) calculated at the Density Functional Theory level. The ground state of all complexes was found to be of high spin, in accordance with the experimental proposal. The calculated structures and vibrational frequencies were also in agreement with experiment, even though comparisons were made with the solid state structure. The calculated nonlinear optical (NLO) properties were for all the compounds analyzed, using the Time Dependent Hartree-Fock (TDHF) method within the static approach, suggesting that these transition metal complexes might be considered as lead molecules to the development of novel based-molecular materials.

Keywords: oxocarbons, coordination compounds, vibrational spectroscopy, nonlinear optical properties, TD-DFT

Introduction

Croconate $(C_5O_5)^{2-}$ is one of the monocyclic ions of the oxocarbon series $[(C_nO_n)^{2-}]$, where the derivatives with n equal to 3-6 constitute the main representatives (Figure 1). These compounds were firstly recognized as a series of molecules by West *et al.*¹ in the 60's. Their structures present D_{nh} symmetry characterized by high degree of electron delocalization around the ring that confers an extra stability to the ionic compounds. For rings larger than five members it has been found² a non-planar form as being more favorable than the D_{nh} isomer. Over the past years, the free oxocarbon ions as well as their

coordination compounds have been widely studied concerning spectroscopic,³⁻⁸ electromagnetic⁹⁻¹² and nonlinear optical properties.¹³⁻¹⁶ Crystallographic structures of the squarate and croconate complexes with first-row transition metals have been described in the literature^{9,17-22} showing molecules with an infinite polymeric chain where the metal ions are surrounded by six oxygen atoms on a distorted octahedron.^{17,18,22} The oxocarbon ion is usually chelated through oxygen atoms to one metal ion and singly-coordinated to another metal, leaving two of its five oxygen atoms (in the case of croconate) uncoordinated. The divalent croconate complexes with $Mn^{2+}, Fe^{2+}, Cu^{2+}, Ni^{2+}, Co^{2+}$ or Zn^{2+} were found to be trihydrated with general formula $M(C_5O_5) \cdot 3H_2O$ and present similar powder X-ray

*e-mail: georgia.junqueira@ufjf.edu.br

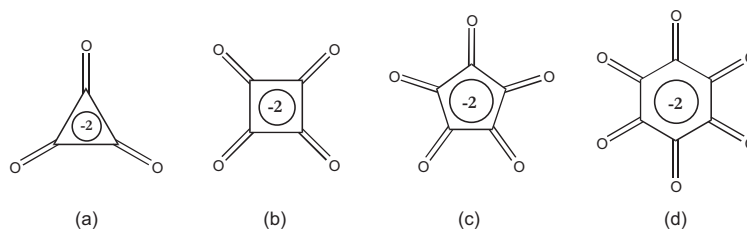


Figure 1. The main oxocarbon representatives: (a) deltate, (b) squarate, (c) croconate, (d) rhodizionate.

diffraction patterns, differing only in the interplanar d-spacing which is often associated to the π -stacking interactions.^{22,23} The magnetic properties of isostructural croconate complexes have been investigated in the last few years.^{17,22} The observed magnetic moments of Mn^{2+} (5.84), Fe^{2+} (5.40), Co^{2+} (5.11), Ni^{2+} (3.26) and Cu^{2+} (1.98 Bohr magnetons) indicate these compounds as high-spin complexes.²² In addition to the interesting chemical physics aspects of these species that have motivated many studies,¹⁻²³ some nonlinear optical applications have also been reported.²⁴ Nonlinear optics (NLO) is associated to the interactions of applied electromagnetic fields in suitable materials to generate new fields altered in frequency or other physical properties. At the molecular level the effect of the light is to polarize the charge distribution and modifies the propagated field. Generally, conjugated molecules asymmetrized by interacting electron donor and acceptor groups are highly polarizable electronic systems with NLO properties. Consequently, the oxocarbon derivatives have already been used as xerographic photoreceptors and their nonlinear optical properties investigated.^{13-16,24} In spite of the extensive literature about oxocarbon species,¹⁻²⁴ the understanding of their coordination compounds at a molecular level is still needed. Our group has used quantum mechanical methods and Monte Carlo simulation to study the oxocarbon ions and their complexes in gas phase and aqueous solution.^{2,25-29} In the present work, we analyze structural, magnetic, spectroscopic and nonlinear optical properties of the coordination compounds of the croconate ion with first-row divalent transition metals with different multiplicities.

Theoretical details

The geometries of the $[\text{M}(\text{C}_5\text{O}_5)(\text{H}_2\text{O})_4]$ ($\text{M} = \text{Mn}^{2+}$, Fe^{2+} , Co^{2+} , Ni^{2+} , Cu^{2+} and Zn^{2+}) compounds were optimized in gas phase at the Density Functional Theory (DFT) level with the BP86 and B3P86^{30,31} functional, employing the standard split-valence basis-set 6-31G(d) and 6-31++G(d,p) for C, O, H atoms and the effective core potential (ECP) LANL2DZ³² for the metal ions. Previous

results by Cundari *et al.*³³ showed that ECP approaches are capable of predicting the geometry of transition metal complexes. The magnetic properties as well as harmonic vibrational frequencies, infrared intensities and Raman activities were also obtained for the complexes at each level of calculation mentioned before.

In this work the hyperpolarizabilities (β) were obtained using the Time Dependent Hartree-Fock (TDHF) method within the static field approach.³⁴⁻³⁶ The TDHF method solves the wave function of the ground electronic state in the presence of the electric field within variational method for the calculation of both static as well as dynamic polarizabilities. The frequency-dependent first hyperpolarizability (dynamic property) is the response of the system at a determinate frequency to oscillatory applied fields, and adds an additional level of complexity in the calculations.³⁵ However, the use of the TDHF within static treatment has produced good results in NLO molecular studies, regarding to the experimental data.³⁷⁻⁴³ The hyperpolarizability tensor β is defined by expanding the dipole moment of a molecule in the presence of an electric field F in a Taylor series (equation 1), where i, j, k, \dots represent x, y, z, \dots and p_i^0 is the dipole moment in the absence of the field, α is the linear polarizability, β is the first hyperpolarizability and γ is the second hyperpolarizability.

$$p = p_i^0 + \alpha_{ij}^0 \cdot F_j + \frac{1}{2!} \beta_{ijk} \cdot F_j F_k + \frac{1}{3!} \gamma_{ijkl} \cdot F_j F_k F_l + \dots \quad (1)$$

For static fields, the hyperpolarizability may be determined as derivative of the induced dipole with respect to the field which may be expressed as a derivative of the energy ϵ with respect to the electric field F (equation 2).

$$\beta = \frac{\partial^2 p}{\partial F^2} = \frac{\partial^2}{\partial F^2} \left(-\frac{\partial \epsilon}{\partial F} \right) = -\frac{\partial^3 \epsilon}{\partial F^3} \quad (2)$$

The β hyperpolarizability is a tensor with 27 components β_{ijk} with $i, j, k = x, y, z$ (Figure 2a). Generally, the nonzero components are reducible due to the symmetry aspects.⁴⁴ For example, if the program code use $\beta_{ijk} = \beta_{ikj}$,

it provides 18 components (Figure 2b). The GAUSSIAN-03⁴⁵ program uses $\beta_{ij}=\beta_{ji}$ hence provides a tensor with only 10 elements (Figure 2c). Concerning the calculation of the total molecular hyperpolarizability (β_{mol}) we reported the three independent values for β as a quasi-Pythagorean problem and solve the complete expression for calculating the magnitude of the total molecular β (equations 3 and 4).⁴⁶ In the present approach, β_{mol} is obtained from the trace elements of the hyperpolarizability tensor, being invariant to an arbitrary rotation of x,y,z axis.³⁴ The calculations were performed with the GAUSSIAN-03 program.⁴⁵

$$\beta_{mol} = (\beta_x^2 + \beta_y^2 + \beta_z^2)^{1/2} \quad (3)$$

$$\beta_i = \frac{1}{3} \sum_{i,k} (\beta_{ikk} + \beta_{kik} + \beta_{kki}) \quad \therefore k = x, y, z; i = x, y, z \quad (4)$$

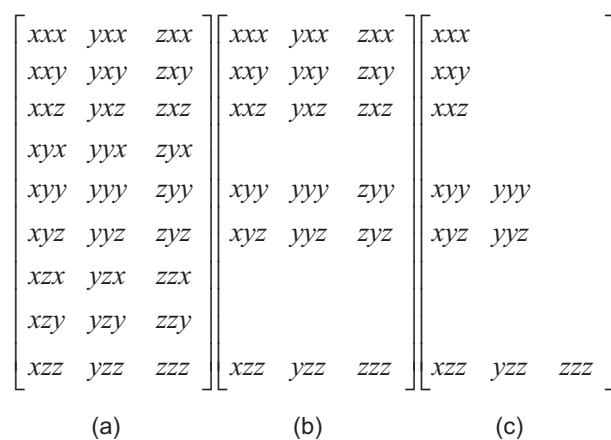


Figure 2. Tensor hiperpolarizability with all components β_{ijk} (a) and only components used in $\beta_{ijk}=\beta_{ikj}$ symmetry (b) and $\beta_{ij}=\beta_{ji}$ symmetry (c).

Results and Discussion

The structures for the croconate complexes with first row transition metals have been described in the literature as a polymeric infinite chain, with two metal ions being coordinated to oxocarbon ligand (Figure 3a). In the present work, the molecular model depicted in Figure 3b was considered with the croconate molecule bond to only one metal ion with a general formula $[M(C_5O_5)(H_2O)_4]$. The

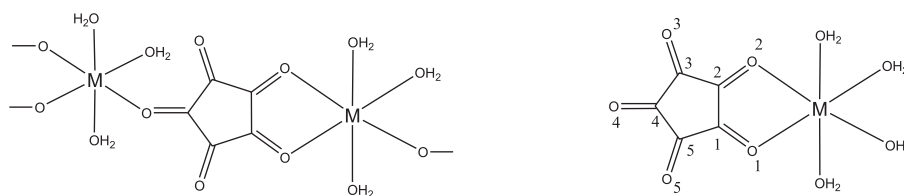


Figure 3. General structure of croconate complexes: (left) solid state arrangement and (right) the model used in the present study.

initial guess was a perfect octahedron and the geometry optimized without any constraint. Distinct electronic states (*i.e.* different multiplicities) were considered and the final optimized geometries are depicted in Figure 4. As can be seen the geometries undergo a significant distortion upon optimization. The relative energy and spin density on the metal center are given in Table 1. It can be observed that the higher spin compounds are the most energetically favorable at both levels of theory studied, except for Fe^{2+} and Ni^{2+} complexes at the BP86 level, where the triplet and singlet states were found as the electronic ground states, respectively. Our results with the B3P86 functional are in better agreement with the magnetic susceptibility and EPR measurements that show the croconate complexes with the divalent metal ions as high-spin species.²³ The determination of the spin density has been used as a criterion to predict molecule-based paramagnetic materials.⁴⁷ The DFT methods have provided good results for both the signs and magnitudes of spin densities at a lower computation cost.⁴⁸ We reported in Table 1 the calculated spin density (ρ) at the metal center for all complexes. The values calculated at the B3P86/6-31++G(d,p) level were found to be quite similar to the B3P86/6-31G(d) ones. In general the spin density is located on the metal ion except for the Cu^{2+} complex, where the single electron is delocalized over the ligand. For this complex the spin-density on the oxygen atoms was found to be 0.132 [B3P86] and 0.077 [BP86] (O1,O2), 0.038 [B3P86] and 0.110 [BP86] (O3,O4,O5), 0.050 [B3P86] and 0.035 [BP86] (water oxygen). The remaining spin-density was found on the other atoms.

As discussed previously, the stability order predicted at B3P86 were in good agreement with the experimental proposal, thus from now on we analyze only the most energetically stable high-spin compounds found at the B3P86 level of theory. The B3P86 calculated structural parameters for the lowest energy high-spin molecules are reported in Table 2 and compared to the experimental X-ray data available.^{22,23,49,50} From the data given in Table 2 it can be noted that the oxocarbon ring presents similar geometry for the whole series, with a short C1-C2 bond (1.39Å), two medium bonds C1-C5 and C2-C3 (~1.46Å) and two longer bond lengths for C3-C4 and C4-C5

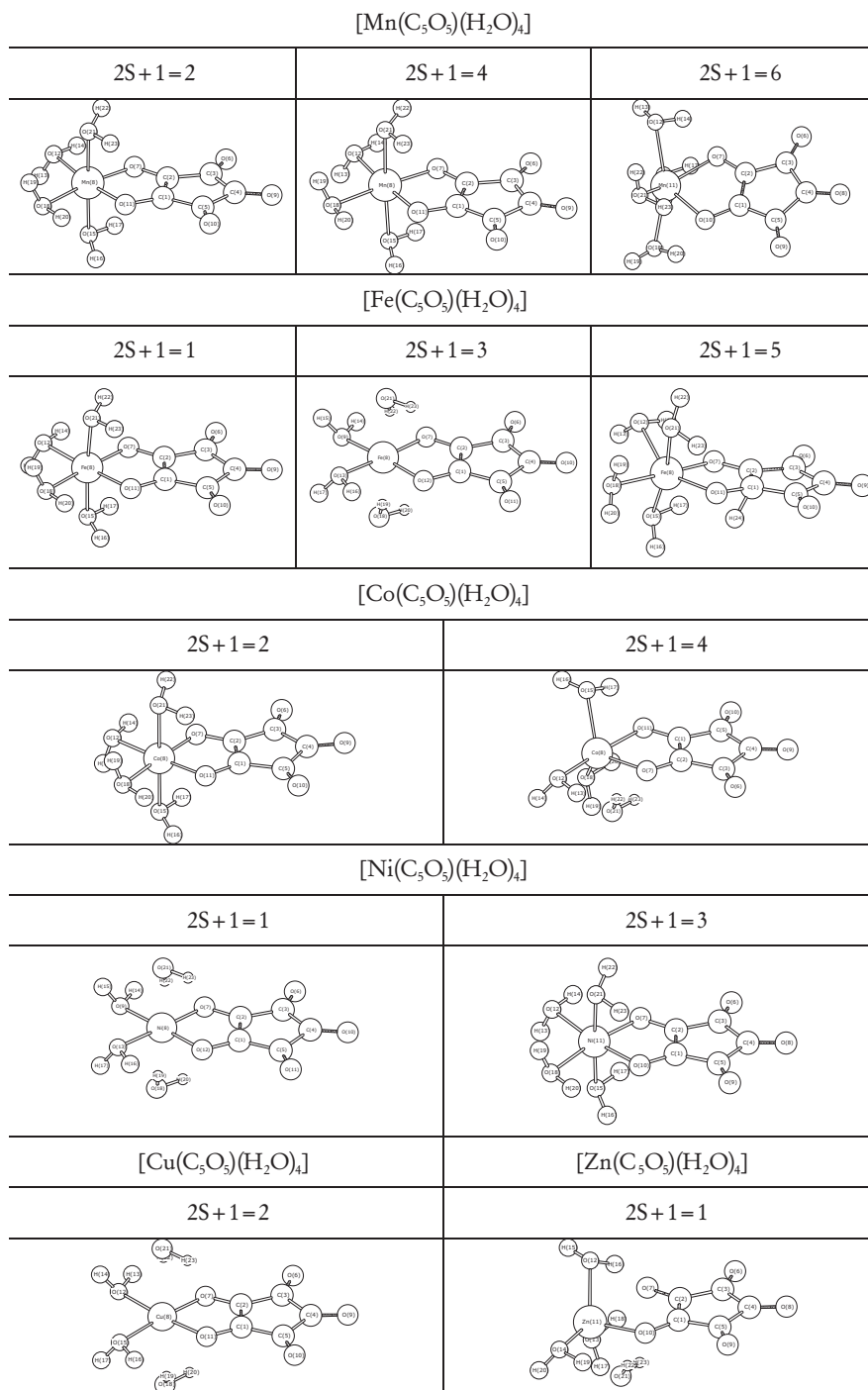


Figure 4. B3P86/6-31G(d) optimized geometries of the croconate complexes.

(~1.53 Å). These characteristics resemble those found for the croconate acid. Experimentally the shortest CC bond was also observed for C1-C2 (~1.44 Å) and the others bond lengths are close to 1.47 Å. The calculated CO bonds are around 1.3 Å for the coordinated groups and 1.2 Å for the free CO moieties. The experimental data show values ranging from 1.18 to 1.27 Å. Therefore the structures of the oxocarbon ring are only slightly dependent on the

metal and molecular multiplicity. In addition, we can see that the coordination geometry strongly depends on the metal type, being the optimized structures found as distorted tetrahedron, quadratic planar and octahedron geometries (Figure 4). The calculated bond length and angles are in good agreement with the experimental findings (Table 2), showing small changes in C-C and C-O bonds in the croconate ring. Considering the free ion

Table 1. Relative energies (ΔE in kcal mol⁻¹) and spin density on the metal center (ρ in atomic units) calculated for the croconate complexes with the first row transition metals. The expected values for \hat{S}^2 are also given in parenthesis

	M=2S+1	BP86/6-31G(d)		B3P86/6-31G(d,p)	
		ΔE	ρ	ΔE	ρ
Mn ²⁺	2	28.5	1.055 (1.12)	48.5	1.039 (1.07)
	4	2.29	2.987 (3.78)	30.7	3.014 (3.76)
	6	0.00	4.733 (8.75)	0.00	4.807 (8.75)
Fe ²⁺	1	20.9	0.000 (0.00)	19.2	0.000 (0.00)
	3	0.00	1.989 (2.02)	2.22	2.040 (2.01)
	5	12.2	3.581 (6.00)	0.00	3.716 (6.00)
Co ²⁺	2	7.23	1.084 (0.89)	15.0	0.9846 (0.78)
	4	0.00	2.528 (3.75)	0.00	2.683 (3.75)
Ni ²⁺	1	0.00	0.000 (0.00)	0.300	0.000 (0.00)
	3	12.9	1.469 (2.00)	0.0	1.624 (2.00)
Cu ²⁺	2	-	0.334 (0.75)	-	0.5163 (0.75)
Zn ²⁺	1	-	0.000 (0.00)	-	0.000 (0.00)

Table 2. Structural parameters calculated for the most stable structures of the croconate complexes at the B3P86/6-31G(d) level of theory. The experimental data are in parenthesis. Bond lengths are in Angstrom and bond angles in degree

	Mn ^a	Fe ^b	Co ^c	Ni	Cu ^d	Zn ^d
M-O1	2.126(2.172)	1.972(2.134)	1.935(2.103)	1.995	1.947(1.970)	2.848(2.116)
M-O2	2.127(2.253)	2.134(2.202)	2.235(2.152)	1.995	1.947 (2.320)	1.962 (2.164)
O1-M-O2	80.4(77.3)	82.4(79.2)	81.6(80.8)	87.6	86.2(81.2)	72.3(80.4)
C1-C2	1.395(1.442)	1.395	1.390(1.437)	1.399	1.389(1.446)	1.393(1.415)
C2-C3	1.466(1.482)	1.468	1.471(1.457)	1.467	1.463(1.457)	1.466(1.480)
C3-C4	1.533(1.472)	1.534	1.537(1.481)	1.532	1.542(1.459)	1.525(1.484)
C4-C5	1.533(1.473)	1.534	1.533(1.466)	1.532	1.542(1.491)	1.533(1.501)
C1-C5	1.466(1.445)	1.463	1.461(1.453)	1.467	1.463 (1.432)	1.474 (1.475)
C1-O1	1.313(1.259)	1.318	1.314(1.256)	1.315	1.306(1.276)	1.320(1.254)
C2-O2	1.313(1.252)	1.309	1.312(1.259)	1.315	1.306(1.244)	1.310(1.247)
C3-O3	1.218(1.180)	1.217	1.216(1.237)	1.218	1.215(1.249)	1.219(1.186)
C4-O4	1.208(1.269)	1.208	1.207(1.248)	1.208	1.204(1.240)	1.208(1.274)
C5-O5	1.218(1.222)	1.218	1.218(1.256)	1.218	1.215(1.243)	1.215(1.217)

^areference 23; ^breference 22; ^creference 49; ^dreference 50.

at the same level of theory, we have found that the average lengths of the C-C and C-O bonds are 1.485 Å and 1.250 Å respectively (Table 2). In the complexation process there is a general trend to increase the C1-O1 and C2-O2 bond lengths (Figure 3), which are directly bound to the metal center, followed by a decreasing in the C1-C2 bond.

The vibrational infrared (IR) and Raman spectra were calculated in gas phase for croconate free ion for the most favorable complexes. The simulated spectra for the complexes are depicted in Figure 5 and the band position and assignments given in Table 3. Looking at Figure 5 it can be seen that the overall profile of the spectra is very similar, except for Cu²⁺ compound, which presented somewhat higher intensities. An explanation for this discrepancy may be attributed from electron super-deslocalization and super-polarization approach.⁵¹ These phenomena are very common when local density approach (LDA) is used, and as a consequence, frequencies and intensity of vibrational transitions are overestimated.⁵²

These effects tend to be partially removed when gradients corrections of the exchange and correlation potentials (GGA) as BP86 and B3P86 functional, are used. It happened for all compound studied, except for the Cu(II) complex, calculated with the B3P86 functional. In this case, the dipole moment (in module) and the polarization values are larger than the ones obtained with the BP86 functional, which can contribute for the Raman intensity overestimation. There is not a clear reason for the strange behavior found for IR and Raman intensities in the Cu²⁺ complex. This may be due the inadequacy of basis-set utilized for metal center, thus it would be worth calculating hyperpolarizabilities for Cu²⁺ complexes using full electron basis-set, such as triple-set 6-311G(d). Our group is engaged in this type of calculation for analogues molecules and the results will be reported soon. For the other complexes the Raman spectra present three absorption bands close to 1790, 1590 and 1390 cm⁻¹ assigned to $\nu(\text{CO})$ and $\nu(\text{CC},\text{CO})$, with the transition

Table 3. B3P86/6-31G(d) vibrational frequencies (in cm^{-1}) and relative intensities for the infrared (in parenthesis) and Raman (in brackets) active modes for the $[\text{M}(\text{C}_5\text{O}_5)(\text{H}_2\text{O})_4]$ transition metal complexes. The experimental data^a, when presente, are also given in brackets

	Mn ²⁺	Fe ²⁺	Co ²⁺	Ni ²⁺	Cu ²⁺	Zn ²⁺	Assignment
IR/R	1789(s)[m]-	1791(s)[m][1722]	1791(s)[m][1723]	1789(s)[m][1724]	1797(s)[w][1723]	1789(s)[m][1725]	$\nu(\text{CO})_{\text{free}}$
IR/R	1595(vs)[s]-	1592(vs)[s][1572]	1598(vs)[s][1580]	1586(vs)[s][1572]	1570(m)[vs]-	1594(vs)[s][1572]	$\nu(\text{CC})+\nu(\text{CO})$
IR	1453(s)	1440(s)	1448(s)	1444(s)	1452(s)	1464(s)	$\nu(\text{CC})+\nu(\text{CO})$
R	-	1426[m]	-	-	1403[s]	-	$\nu(\text{CC})+\nu(\text{CO})$
IR/R	1387(w)[m]	1396(w)[m][1229]	1398(m)[m][1231]	1379(w)[m][1229]	-[1227]	1390(w)[m][1231]	$\nu(\text{CC})$
IR	1152(w)	1160(w)	1155(w)	-	1169(w)	1160(w)	$\nu(\text{CC})$
IR/R	1082(m)[w]	1072(m)[vw]	1080(m)[vw]	1076(m)[vw]	1032(w)[vs]	1085(m)[w]	$\nu(\text{CC})$
IR/R	630(m)[w]-	653(w)[vw][653]	639(m)[vw][640]	632(w)[vw][654]	639(w)[w][641]	633(m)[vw][653]	ring breath.
IR	575(m)	581(w)	563(w)	-	574(w)	561(w)[w]	ring
R	549[w]-	523[w][564]	569[w][564]	546[w][561]	543[vs][562]	550[w][561]	δ ring
IR/R	552(m)[vw]	551(w)[w]	561(w)[w]	546(w)[w]	516(w)[w]	517(w)[vw]	δ ring
R	346[w]	-	-	-	-	-	δ CO
IR	317(w)	350(w)	342(m)	338(m)	333(m)[m]	351(m)	δ CO
IR	283(w)	254(w)[w]	293(w)[w]	296(w)	310(w)	287(w)	δ CO _{free}

^areference 8.

around 1590 cm^{-1} found to be more intense. The highest frequency mode at $\sim 1790 \text{ cm}^{-1}$ was assigned to the stretching of the uncoordinated CO groups. These calculated transitions are in good agreement with the experimental data, which show absorption bands at ~ 1720 , 1570 and 1230 cm^{-1} .⁸ The theoretical values are overestimated compared to the observed ones by an average factor of 0.94 that is close to common scaling factors used for vibrational frequencies at the DFT level.⁵¹ For the $[\text{Fe}(\text{C}_5\text{O}_5)(\text{H}_2\text{O})_4]$ complex two medium intensity absorptions were calculated at 1426 and 1396 cm^{-1} , attributed to the $\nu(\text{CC},\text{CO})$ mode. The 1200 - 200 cm^{-1} region presented only weak absorptions in the Raman spectra assigned to the ring breathing ($\sim 640 \text{ cm}^{-1}$) and ring deformation ($\sim 550 \text{ cm}^{-1}$). The experimental data in this region are around 650 and 560 cm^{-1} supporting our calculations. The IR spectra present four distinct regions: 2000 - 1400 cm^{-1} , 1200 - 800 cm^{-1} , 700 - 500 cm^{-1} and 400 - 200 cm^{-1} assigned to $\nu(\text{CO})$, $\nu(\text{CC})$, $\delta(\text{ring})$ and $\delta(\text{CO})$ modes respectively. As in the Raman spectra the most intense transitions were assigned as $\nu(\text{CO})$ and $\nu(\text{CC},\text{CO})$ and found close to 1790 , 1590 and 1450 cm^{-1} . The pure $\nu(\text{CC})$ stretching appeared at 1395 and 1080 cm^{-1} , with small variation throughout the series. The modes associated to the whole oxocarbon ring were at ~ 650 and 550 cm^{-1} and the $\delta(\text{CO})$ vibration was calculated at 340 cm^{-1} . In general the experimental and theoretical data suggest that the D_{3h} symmetry of croconate is reduced to C_{2v} after coordination.

In the last part of this paper the NLO properties are analyzed. The central aim of calculating molecular NLO quantities is to predict β and γ for chemical systems.⁴⁶ Nonlinear optical properties are of interest due to their potential application to optical devices, as frequency-

doubling devices, optical signal processing and optical computers.⁴⁶ Molecules with NLO applications, in general, contain high values of molecular hyperpolarizabilities (β) and permanent dipole moments (μ) beside the fact that they must be transparent in the second-order harmonic generation (SHG) region to avoid re-absorption of the converted light.⁴⁶ Recently, transition metal organometallic and coordination complexes have emerged as potential application for second-order NLO materials.^{33,53} Compared to organic molecules, metal complexes offer a larger variety of structures, oxidation and spin states that enhance NLO properties. In general the values of the molecular hyperpolarizabilities (β) are considered moderate (1 - 10), high (10 - 100) or very high (above $100 \times 10^{-30} \text{ cm}^5/\text{e.s.u}$) for nonlinear applications.⁴⁶ In the present paper the molecular hyperpolarizabilities (β_{mol}) were calculated in gas phase for the croconate free ion and for the most favorable complexes optimized at B3P86 level of theory employing basis set with inclusion of polarization and diffuse functions [6-31G(d), 6-31++G(d,p)] on the O, C and H atoms⁵⁴ and effective core potential (ECP) LANL2DZ³² for the metal transition ions (Table 4). Usually the quality of the basis set is very important in obtaining accurate NLO properties being the size required much larger than those used in normal energy and structure calculations, in order to adequately describe the induced polarization of electrons.^{33,46,55} Extensive researches for organic molecules suggest that the improvement of basis-set is usually more important than the electronic correlation effect for accurate calculations of NLO properties.^{46,56,57} Analyzing the values in Table 4 it can be noted that the inclusion of diffuse functions on the 6-31G(d) basis set in the calculations leads to larger hyperpolarizabilities as well as dipole moments. For the

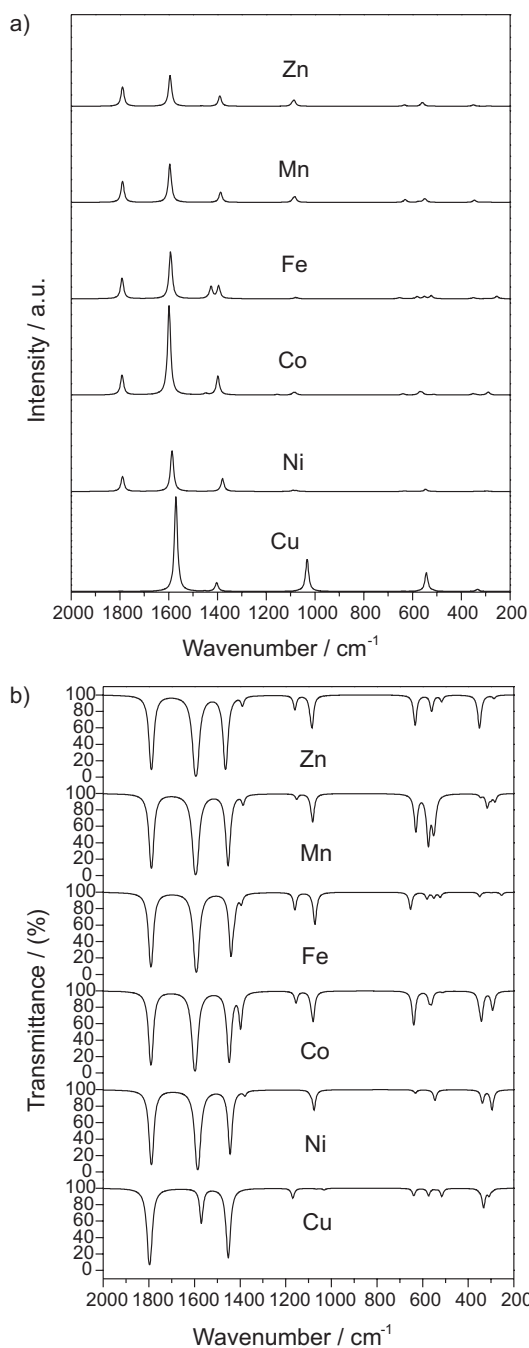


Figure 5. B3P86/6-31G(d) Raman (a) and infrared (b) simulated spectra for the croconate complexes.

compounds studied the β values ranged from 0.530 to $51.3 \times 10^{-30} \text{ cm}^5/\text{e.s.u.}$ [6-31G(d)] and from 2.13 to $73.9 \times 10^{-30} \text{ cm}^5/\text{e.s.u.}$ [6-31++G(d,p)] for Mn^{2+} and Cu^{2+} coordination compounds respectively. For the Mn^{2+} complex the molecular hyperpolarizability (β_{mol}) value increased 300% with the 6-31++G(d,p) basis set ($2.13 \times 10^{-30} \text{ cm}^5/\text{e.s.u.}$) compared to the 6-31G(d) result ($0.530 \times 10^{-30} \text{ cm}^5/\text{e.s.u.}$). For the other complexes the β_{mol} value increased about 100% [Ni^{2+}]; 70% [Fe^{2+} , Co^{2+}]; 40% [Cu^{2+}]

Table 4. B3P86 hyperpolarizabilities ($\beta_{\text{mol}}/10^{-30} \text{ cm}^5/\text{e.s.u.}$) and dipole moments (μ/D) calculated for the free anion croconate and its complexes with the first row transition metals

	B3P86/6-31G(d)		B3P86/6-31++G(d,p)	
	β_{mol}	μ	β_{mol}	μ
Free	0.02	0.00	0.00	0.00
Mn^{2+}	0.530	14.2	2.13	15.9
Fe^{2+}	0.910	13.7	1.57	15.2
Co^{2+}	2.43	13.4	4.06	16.1
Ni^{2+}	0.610	12.7	1.22	14.7
Cu^{2+}	51.3	11.5	73.9	12.5
Zn^{2+}	2.07	14.5	2.27	16.3

and around 10% for Zn^{2+} complex, with the addition of diffuse functions. Despite the difference in the absolute values, the general trend behavior is the same at both levels of theory considered. It is important to point out that the hyperpolarizabilities found here were quite sensitive to the structure and electronic properties of the studied compounds. Our main goal here was to analyze the hyperpolarizability of the croconate complexes with different coordinated metals. Other interesting behavior is observed for the hyperpolarizability, with β decreasing with the spin density on the metal center for the paramagnetic compounds from 51.3 ($\rho(\text{Cu})=0.5$) to $0.5 \times 10^{-30} \text{ cm}^5/\text{e.s.u.}$ ($\rho(\text{Mn})=4.8$) at the B3P86/6-31G(d) level. The exception is the Ni^{2+} complex that shows a spin density of 1.6 and β equal to $0.61 \times 10^{-30} \text{ cm}^5/\text{e.s.u.}$ [6-31G(d) value]. In that case the total spin density is centered on the metal atom, differing from the Cu^{2+} compound, where it is spread over the oxocarbon ring. Therefore, the delocalized spin density seems to be important to enhance the hyperpolarizability and then might be considered as an important parameter to design molecules with potential application in NLO devices.

Conclusions

In the present work we employed standard quantum mechanical methods to calculate gas phase structural and spectroscopic properties of transition metal complexes with croconate oxocarbon ion, by means of theoretical DFT framework. Our results were found in good agreement with the experimental observed spectra and X-ray data. A very interesting outcome from our paper showed the high-spin species as more stable in gas phase, in agreement with EPR analysis. The structure of the oxocarbon ring was slightly dependent on the metal and molecular multiplicity, which is also supported by experimental finding. Additionally, we studied NLO properties of the croconate complexes using TDHF static

approach. We stated that the molecular hyperpolarizability (β_{mol}) as well as the dipole moment (μ) values were dependent on the metal coordinated. The reported values showed that the inclusion of diffuse functions on the basis-set leads to substantially larger β_{mol} values. Interestingly the hyperpolarizability calculated for Cu(II) complex was $51.3 \times 10^{-30} \text{ cm}^5/\text{e.s.u}$ [B3P86/6-31G(d)] and $73.9 \times 10^{-30} \text{ cm}^5/\text{e.s.u}$ [B3P86/6-31++G(d,p)] showing this molecule as potential lead compound in the development of novel NLO molecular-based materials. The β values were found to be correlated with the spin density on the molecule, with complexes having high spin density on the metal center generating lower β values.

Acknowledgments

The authors would like to thank the FAPEMIG (Fundação de Amparo à Pesquisa do Estado de Minas Gerais), CNPq (Conselho Nacional de Desenvolvimento Científico e Tecnológico) and PROPESQ (Pró-Reitoria de Pesquisa da Universidade Federal de Juiz de Fora) for financial support. G. M. A. Junqueira is also grateful to CNPq Brasil, for the research scholarship.

References

1. West, R.; Niu, H. Y.; Powell, D. L.; Evans, M. V.; *J. Am. Chem. Soc.* **1960**, *82*, 6204.
2. Junqueira, G. M. A.; Rocha, W. R.; De Almeida, W. B.; Dos Santos, H. F.; *THEOCHEM* **2004**, *684*, 141.
3. Soula, B.; Galibert, A.; Donnadiou, B.; Fabre, P.; *Inorg. Chim. Acta* **2001**, *324*, 90.
4. Ito, M.; West, R.; *J. Am. Chem. Soc.* **1963**, *85*, 2580.
5. Lopes, J. G. S.; de Oliveira, L. F. C.; Santos, P. S.; *Spectrochim. Acta, Part A* **2001**, *57*, 399.
6. Ribeiro, M. C. C.; de Oliveira, L. F. C.; Santos, P. S.; *Chem. Phys.* **1997**, *217*, 71.
7. West, R.; Eggerding, D.; Perkins, J.; Handy, D.; Tuazon, E. C.; *J. Am. Chem. Soc.* **1979**, *101*, 1710.
8. Santos, P. S.; Amaral, J. H.; de Oliveira, L. F. C.; *J. Mol. Struct.* **1991**, *243*, 223.
9. Deguenon, D.; Bernadinelli, G.; Tuchagues, J. P.; Castan, P.; *Inorg. Chem.* **1990**, *29*, 3031.
10. Bernadinelli, G.; Deguenon, D.; Soules, R.; Castan, A.; *Can. J. Chem.* **1989**, *67*, 1158.
11. Van Ooijen, J. A. C.; Reedijk, J.; Spek, A. L.; *Inorg. Chem.* **1979**, *18*, 1184.
12. Habenschuss, M.; Gerstein, B. C.; *J. Chem. Phys.* **1974**, *61*, 852.
13. Chen, C.; Marder, S. R.; Cheng, L.; *J. Am. Chem. Soc.* **1994**, *116*, 3117.
14. Law, K.; *J. Phys. Chem.* **1995**, *99*, 9818.
15. Morley, J. O.; *THEOCHEM* **1995**, *357*, 49.
16. Spassova, M.; Kolev, T.; Kanev, I.; *THEOCHEM* **2000**, *528*, 151 and cited references.
17. Cornia, A.; Fabretti, A. C.; Giusti, A.; Ferraro, F.; Gatteschi, D.; *Inorg. Chim. Acta* **1993**, *212*, 87.
18. Glick, M. D.; Dahl, L. F.; *Inorg. Chem.* **1966**, *5*, 289.
19. Castan, P.; Deguenon, D.; Dahan, F.; *Acta Crystallogr., Sect. A: Found. Crystallogr.* **1991**, *47*, 2656.
20. Castro, I.; Sletten, J.; Faus, J.; Julve, M.; *J. Chem. Soc. Dalton Trans.* **1992**, 2271.
21. Castro, I.; Sletter, J.; Faus, J.; Julve, M.; Journaux, Y.; Lloret, F.; Alvarez, S.; *Inorg. Chem.* **1992**, *31*, 1889.
22. West, R.; Niu, H. Y.; *J. Am. Chem. Soc.* **1963**, *85*, 2586.
23. Georgopoulos, S. L.; Diniz, R.; Yoshida, M. I.; Speziali, N. L.; Dos Santos, H. F.; Junqueira, G. M. A.; de Oliveira, L. F. C.; *J. Mol. Struct.* **2006**, *794*, 63.
24. Seitz, G.; Imming, P.; *Chem. Rev.* **1992**, *92*, 1227 and references cited herein.
25. Junqueira, G. M. A.; Rocha, W. R.; De Almeida, W. B.; Dos Santos, H. F.; *Phys. Chem. Chem. Phys.* **2001**, *3*, 3499.
26. Junqueira, G. M. A.; Rocha, W. R.; De Almeida, W. B.; Dos Santos, H. F.; *Phys. Chem. Chem. Phys.* **2002**, *4*, 2517.
27. Junqueira, G. M. A.; Rocha, W. R.; De Almeida, W. B.; Dos Santos, H. F.; *Phys. Chem. Chem. Phys.* **2002**, *4*, 2919.
28. Junqueira, G. M. A.; Rocha, W. R.; De Almeida, W. B.; Dos Santos, H. F.; *Phys. Chem. Chem. Phys.* **2003**, *5*, 437.
29. Junqueira, G. M. A.; Rocha, W. R.; De Almeida, W. B.; Dos Santos, H. F.; *THEOCHEM* **2005**, *719*, 31.
30. Perdew, J. P.; *Phys. Rev. B: Condens. Matter Mater. Phys.* **1986**, *33*, 8822.
31. Becke, A. D.; *Phys. Rev. A: At., Mol., Opt. Phys.* **1988**, *38*, 3098.
32. Hay, P. J.; Wadt, W. R.; *J. Chem. Phys.* **1985**, *82*, 299.
33. Cundari, T. R.; Kurtz, H. A.; Zhov, T.; *J. Phys. Chem. A* **1998**, *102*, 2962.
34. Sequino, H.; Bartlett, R.; *J. Chem. Phys.* **1986**, *85*, 976.
35. Rice, J. E.; Amos, R. D.; Colwell, S. M.; Handy, N. C.; Sanz, J.; *J. Chem. Phys.* **1990**, *93*, 12.
36. Dupuis, M.; Karna, S.; *J. Comput. Chem.* **1991**, *12*, 487.
37. Moura, G. L.; Simas, A. M.; Miller, J.; *Chem. Phys. Lett.* **1996**, *257*, 639.
38. Bezerra Jr., A. G.; Gomes, A. S. L.; Athayde-Filho, P. F.; da Rocha, G. B.; Miller, J.; Simas, A. M.; *Chem. Phys. Lett.* **1999**, *309*, 421.
39. Machado, A. E. A.; Gama, A. A. S.; *THEOCHEM* **2003**, *620*, 21.
40. Hillebrand, S.; Segala, M.; Backup, T.; Correia, R. R. B.; Horowitz, F.; Stefani, V.; *Chem. Phys.* **2001**, *273*, 1.
41. Rodembusch, F. S.; Backup, T.; Segala, M.; Tavares, L.; Correia, R. R. B.; Stefani, V.; *Chem. Phys.* **2004**, *305*, 115.

42. Machado, A. E.; Neto, B. B.; Gama, A. A. S.; *J. Comput. Meth. Sci. Eng.* **2004**, *4*, 267.
43. Silva, A. M.; Rocha, G. B.; Menezes, P. H.; Miller, J.; Simas, A. M.; *J. Braz. Chem. Soc.* **2005**, *16*, 583.
44. Kleinman, D. A.; *Phys. Rev.* **1977**, *126*, 1962.
45. *Gaussian 03, Revision B.05*, Frisch, M. J.; Trucks, G. W.; Schlegel, H. B.; Scuseria, G. E.; Robb, M. A.; Cheeseman, J. R.; Montgomery Jr., J. A.; Vreven, T.; Kudin, K. N.; Burant, J. C.; Millam, J. M.; Iyengar, S. S.; Tomasi, J.; Barone, V.; Mennucci, B.; Cossi, M.; Scalmani, G.; Rega, N.; Petersson, G. A.; Nakatsuji, H.; Hada, M.; Ehara, M.; Toyota, K.; Fukuda, R.; Hasegawa, J.; Ishida, M.; Nakajima, T.; Honda, Y.; Kitao, O.; Nakai, H.; Klene, M.; Li, X.; Knox, J. E.; Hratchian, H. P.; Cross, J. B.; Adamo, C.; Jaramillo, J.; Gomperts, R.; Stratmann, R. E.; Yazyev, O.; Austin, A. J.; Cammi, R.; Pomelli, C.; Ochterski, J. W.; Ayala, P. Y.; Morokuma, K.; Voth, G. A.; Salvador, P.; Dannenberg, J. J.; Zakrzewski, V. G.; Dapprich, S.; Daniels, A. D.; Strain, M. C.; Farkas, O.; Malick, D. K.; Rabuck, A. D.; Raghavachari, K.; Foresman, J. B.; Ortiz, J. V.; Cui, Q.; Baboul, A. G.; Clifford, S.; Cioslowski, J.; Stefanov, B. B.; Liu, G.; Liashenko, A.; Piskorz, P.; Komaromi, I.; Martin, R. L.; Fox, D. J.; Keith, T.; Al-Laham, M. A.; Peng, C. Y.; Nanayakkara, A.; Challacombe, M.; Gill, P. M. W.; Johnson, B.; Chen, W.; Wong, M. W.; Gonzalez, C.; Pople, J. A.; Gaussian, Inc.: Pittsburgh PA, 2003.
46. Kanis, D. R.; Ratner, M. A.; Marks, T. J.; *Chem. Rev.* **1994**, *94*, 195 and references cited herein.
47. Zheludev, A.; Barone, V.; Bonnet, M.; Delley, B.; Grand, A.; Ressouche, E.; Rey, P.; Subra, R.; Schweizer, J.; *J. Am. Chem. Soc.* **1994**, *116*, 2019.
48. Yamanaka, S.; Kawakami, T.; Yamada, S.; Nagao, H.; Nakano, M.; Yamaguchi, K.; *Chem. Phys. Lett.* **1995**, *240*, 268.
49. Dumestre, F.; Soula, B.; Galibert, A. M.; Fabre, P. L.; Bernardinelli, G.; Donnadiou, B.; Castan, P.; *J. Chem. Soc. Dalton Trans.* **1998**, 4131.
50. Glick, M. D.; Dows, G. L.; Dahl, L. F.; *Inorg. Chem.* **1964**, *12*, 1712.
51. Wang, J.; Eriksson, L. A.; Boyd, R. J.; Shi, Z.; Johnson, B. G.; *J. Phys. Chem.* **1994**, *98*, 1844.
52. Morgon, N. H.; Custódio, R.; *Quim. Nova* **1995**, *18*, 44.
53. Liyanage, P. S.; Silva, R. M.; Silva, K. M. N.; *THEOCHEM* **2003**, *639*, 195.
54. Krishnan, R.; Binkley, J. S.; Seeger, R.; Pople, J. A.; *J. Chem. Phys.* **1980**, *72*, 650; McLean, A. D.; Chandler, G. S.; *J. Chem. Phys.* **1980**, *72*, 5639; Clark, T.; Chandrasekhar, J.; Spitznagel, G. W.; Schleyer, P.V.R.; *J. Comput. Chem.* **1983**, *4*, 294; Frisch, M. J.; Pople, J. A.; Binkley, J. S.; *J. Chem. Phys.* **1984**, *80*, 3265.
55. Brédas, J. L.; Adant, C.; Tackx, P.; Persoons, A.; *Chem. Rev.* **1994**, *94*, 243.
56. Hobza, P.; Selzle, H. L.; Schlag, E. W.; *Chem. Rev.* **1994**, *94*, 1767.
57. Dykstra, C. E.; *Studies in Physical and Theoretical Chemistry*, Elsevier: Amsterdam, 1998, v. 58.

Received: November 16, 2006

Web Release Date: November 12, 2007